

ErAs:(InGaAs)_{1-x}(InAlAs)_x alloy power generator modules

Gehong Zeng,^{a)} Je-Hyeong Bahk, and John E. Bowers

Department of Electrical and Computer Engineering, University of California, Santa Barbara, California 93106, USA

Joshua M. O. Zide and Arthur C. Gossard

Materials Department, University of California, Santa Barbara, California 93106, USA

Zhixi Bian, Rajeev Singh, and Ali Shakouri

Electrical Engineering Department, University of California, Santa Cruz, California 95064, USA

Woochul Kim

School of Mechanical Engineering, Yonsei University, Seoul 120-749, Korea

Suzanne L. Singer and Arun Majumdar

Department of Mechanical Engineering, University of California, Berkeley, California 94720, USA

(Received 3 August 2007; accepted 4 December 2007; published online 27 December 2007)

We report a wafer scale approach for the fabrication of 400 element power generator modules composed of 200 *n*-type ErAs:(InGaAs)_{0.8}(InAlAs)_{0.2} and 200 *p*-type ErAs:InGaAs alloy thermoelectric elements. The thermoelectric properties of the materials were characterized. Two sets of generator modules with the element thicknesses of 20 and 10 μm , respectively, were fabricated. The 20 μm module had an output power density of 2.5 W/cm² and 3.5 V open circuit voltages, and the 10 μm generator modules had an output power density of 1.12 W/cm² and open circuit voltage of 2.1 V. The performance of thermoelectric generator modules can further be improved by increasing the thicknesses of the elements and reducing the electrical and thermal parasitic resistances. © 2007 American Institute of Physics. [DOI: 10.1063/1.2828042]

Solid state thermoelectric generator modules operating at temperatures near room temperature (300–600 K) with high efficiencies (>10%–20%) are of great interest. Applications range from waste heat recovery of land and sea vehicles to deep space exploration.¹ The output power and efficiency of a thermoelectric generator module depend largely on the material's thermoelectric properties, which are often summarized with the figure of merit, $ZT = \alpha^2 \sigma T / \kappa$, where α , σ , κ and T are the Seebeck coefficient, electrical conductivity, thermal conductivity and absolute temperature, respectively. Thermoelectric properties can be improved by introducing nanometer scale structure into materials.² In this way, the Seebeck coefficient can be increased through thermionic emission,^{3–5} and the thermal conductivity can be reduced due to the increase of phonon interface scattering.⁶ Thermal conductivity reduction using superlattice heterostructures or incorporation of nanoparticles has been demonstrated.^{7–9} Much of the recent ZT improvements come mainly from the reduction of thermal conductivity. In our study, ErAs nanoparticles, a rocksalt semimetal nanostructure, were epitaxially incorporated into (InGaAs)_{1-x}(InAlAs)_x using molecular beam epitaxy (MBE). The ErAs nanoparticles in the InGaAlAs can provide both charge carriers and create phonon scattering centers. Experiments show that the ErAs nanoparticles form effective phonon scattering centers for middle and long wavelength phonons, and therefore the thermal conductivity can be reduced.¹⁰ The combination of a large Seebeck coefficient, low thermal conductivity, and possibly high electrical conductivity can dramatically improve the material's figure of merit Z .

Low output voltage and low output power have been a problem for thermoelectric generators. Solid state generator modules with output power in watts and output voltage in volts are needed in most real applications and this drove our research in solid state generator modules using ErAs:(InGaAs)_{1-x}(InAlAs)_x alloy elements. In this paper, we report 400 element generator modules of 20 or 10 μm thick (InGaAs)_{1-x}(InAlAs)_x alloy embedded with ErAs nanoparticles. An output power density of 2.5 and 1.12 W/cm² were measured for these 20 and 10 μm generator modules, respectively.

The ErAs:(InGaAs)_{1-x}(InAlAs)_x samples were grown using a Varian Gen II molecular beam epitaxy system on lattice matched (100) InP substrates with a cap and a buffer layer of 250 nm doped InGaAs.^{11–13} The doped cap and buffer layers were used as contact layers for low metallization contact resistance. The InGaAlAs epitaxial layer consists of a digital alloy of 80% InGaAs and 20% InAlAs with 0.3% erbium arsenide.

One aspect of incorporating ErAs nanoparticles is to reduce the thermal conductivity below that of InGaAs or InGaAlAs. It has been shown previously that incorporating ErAs nanoparticles 1–5 nm in diameter effectively reduces the thermal conductivity below InGaAs because ErAs nanoparticles effectively scatter long and middle wavelength phonons while atomic substitution in InGaAs alloy scatters short wavelength phonons.¹⁰ Thermal conductivity of (InGaAs)_{0.8}(InAlAs)_{0.2} with 0.3% ErAs nanoparticles was measured at University of California at Berkeley (UCB) using the 3ω method (Fig. 1). When ErAs nanoparticles are incorporated into (InGaAs)_{1-x}(InAlAs)_x, potential barriers are formed at the interface between the particle and semiconductor. The Seebeck coefficient can be enhanced through the

^{a)}Electronic mail: gehong@ece.ucsb.edu

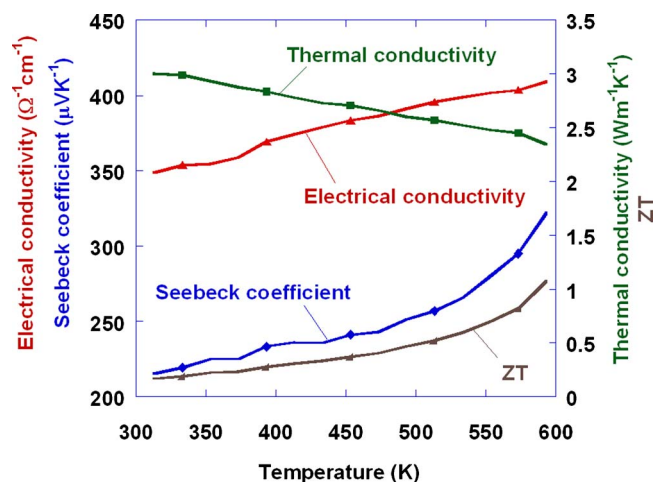


FIG. 1. (Color online) The thermal conductivity, electrical conductivity, Seebeck coefficient, and ZT of *n*-type ErAs:InGaAlAs.

electron filtering effects of these potential barriers.¹⁴

Samples with epitaxial layers of 0.3% ErAs:(InGaAs)_{0.8}(InAlAs)_{0.2} with 0.5 and 2 μm thickness, respectively, were grown on semi-insulating InP substrates using MBE for the Seebeck coefficient and electrical conductivity measurements. The 2 μm epitaxial layer samples were processed for Seebeck coefficient measurements. The test chips were coated with 300 nm Si₃N₄. Different test samples from the same material wafer were measured separately at both the University of California at Santa Barbara (UCSB) and the University of California at Santa Cruz (UCSC) to ensure that measurements were carried out properly. The results shown in Fig. 1 are an average of the two measurements.

Epitaxial layer samples 0.5 μm thick were used for van der Paw measurements. The sample was coated with 300 nm Si₃N₄ as a passivation layer. The measurements were carried out in vacuum around 1 × 10⁻³ Torr. The test chips from the same wafer sample were measured at UCSC, UCSB, and Jet Propulsion Laboratory.

The figure of merit ZT value for InGaAs or InGaAlAs bulk material is around 0.02–0.05 at room temperature.^{15,16} By incorporating ErAs nanoparticles, the ZT value of ErAs:InGaAlAs is increased to 0.16 at room temperature due to the reduction of thermal conductivity and the enhancement in Seebeck coefficient. The ZT value keeps increasing with the temperature (Fig. 1). The thermoelectric properties of the material above 600 K are still under investigation.

ErAs:InGaAlAs generator modules were fabricated via a wafer scale approach using processing techniques similar to those of standard large scale integrated circuits, and generator modules were bonded using flip-chip bonding techniques. The element mesas were formed using inductively coupled plasma dry etching with a gas ratio of Cl₂/N₂/Ar₂ = 20/40/2 SCCM (SCCM denotes cubic centimeter per minute at STP) at 200 °C. After all mesas were formed, contact metal and metal barrier layers were deposited on top of these mesas and then the *n*- and *p*-type wafers were diced into square chips for bonding, each chip containing 200 elements.

Connection metal pads of Ti/Au were deposited on the AlN plates using an electron beam evaporator. The 200 element *n*-type chip was bonded to a lower AlN plate, and the 200 element *p*-type chip was bonded to an upper AlN plate

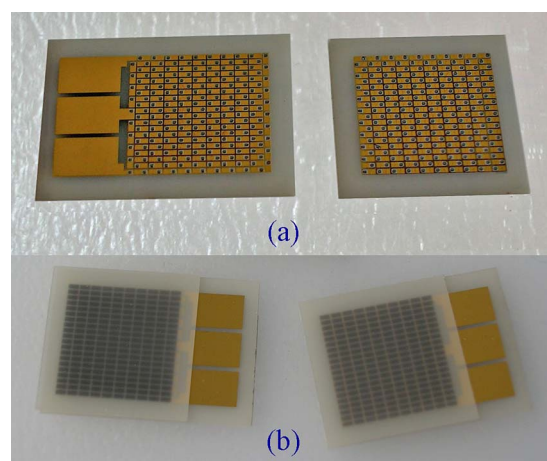


FIG. 2. (Color online) (a) 200 *n*-type elements of ErAs:(InGaAs)_{0.8}(InAlAs)_{0.2} and 200 *p*-type elements of ErAs:(InGaAs) were bonded on a lower and upper AlN plate. (b) Two 400 element generator modules.

via flip chip bonding. After the InP substrate 520 μm thick was removed using a HCl solution, the 200 epitaxial elements of 10 or 20 μm sample were left bonded on the AlN plates. Finally, the lower AlN plate bonded with 200 *n*-type elements and the upper AlN plate bonded with 200 *p*-type elements were bonded together using flip-chip bonding again to form a 400 element generator module. Figure 2 shows the lower and upper AlN plates bonded with 200 *n*-type elements and 200 *p*-type elements, respectively, and two fabricated 400 element generator modules packaged with AlN plates 125 μm thick.

In our experiments, organic residues on the surface were removed via ultraviolet ozone, and ammonia solutions were used for surface oxide film cleaning. After ammonia solution treatment, the sample surface was still kept in an ammonia environment to prevent it from being exposed to air. Thus, truly clean surfaces were achieved for low contact resistance. Transmission line method patterns were fabricated, and the

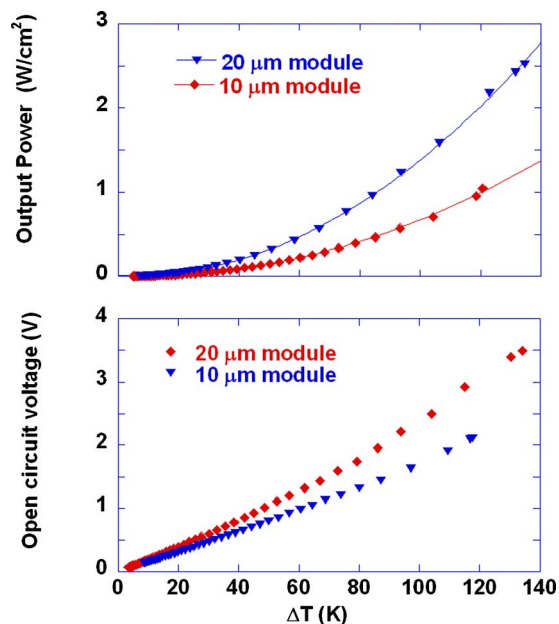


FIG. 3. (Color online) Open circuit voltage and output power measured for 10 and 20 μm generator modules.

TABLE I. Comparison of the electrical loss from Ohmic contact and connection metal pad resistance for 400 element 10 and 20 μm generator modules. The Au pads are 6 μm thick for 10 μm generator modules and 10 μm thick for 20 μm generator modules.

Element thickness (μm)	Element resistance (Ω)	Contact resistance (Ω)	Metal pad resistance (Ω)	Parasitic loss (%)
10	11	5	3	42
20	22	5	2	24

specific contact resistance on the order of $10^{-7} \Omega \text{cm}^2$ for both *n*- and *p*-type materials was measured.

The internal resistance *r* for 10 μm modules was 19 Ω , and the internal resistance was typically 29 Ω for 20 μm modules at room temperature. An open circuit voltage of 2.1 V and output power of 1.12 W/cm^2 were measured for 10 μm generator modules with a temperature difference up to 120 K built up across the generator modules, while open circuit voltage of 3.5 V and output power 2.5 W/cm^2 were measured for 20 μm generator modules with 140 K temperature difference across the modules (Fig. 3).

The electrical parasitic loss comparison between our 400 element 10 μm generator modules and 20 μm generator modules is given in Table I, which shows the electrical loss from contact and connection metal resistance is about 42% for 10 μm generator modules, but the value is reduced to 24% when the element thickness is increased to 20 μm . The electrical parasitic loss could be reduced to around 5% only by increasing the element thickness to 120 μm . The temperature difference across the generator elements $\Delta T_{\text{element}}$ is another issue. The $\Delta T_{\text{element}}$ has to be substantially increased for high output power and high efficiency. For thin film generators, the heat flux through the generator elements can be so high that heat transfer coefficient of the heat sink using present cooling techniques can become a major limitation of the performance. The heat flux from the generator to the heat sink can be reduced to some degrees through the heat spreading from the generator element to the heat sink. Properly increasing the thickness of generator is a solution and has some advantages: (i) effectively reduce the heat flux from the generator elements to heat sink; (ii) output power and efficiency can be enhanced due to the increase of temperature difference across the elements. The average temperature difference across the elements $\Delta T_{\text{element}}$ for the 10 μm generator module was estimated to be about 24 K and the value was increased to around 39 K for the 20 μm generator modules. The performance of the 20 μm generator modules was improved accordingly: the open circuit voltage increased from 2.1 to 3.5 V, the output power was increased from 1.12 to 2.5 W/cm^2 , and the electric parasitic loss from contact resistance and connection metals was also reduced from 42% to 24%.

Solid state thermoelectric generators are desirable for long life, robustness, compact size, light weight, and high

reliability, which are important for space explorations, where the heat dissipation on the cold side largely depends on radiation, so the generator must have low heat flux from heat source to heat sink, and large temperature drop across the elements is required to achieve desirable output power and conversion efficiency. Thick bulk material with good high temperature thermoelectric properties will become necessary. One of the significant advantages of the ErAs:InGaAs material system is that it provides a viable way to a thermoelectric material which can be produced using bulk synthesis, because ErAs nanoparticles are thermodynamically stable in III-V semiconductors such as InGaAs.¹⁷ The ErAs:InGaAs and ErAs:InGaAlAs growth using bulk synthesis is now underway. With further improvements on material thermoelectric properties, processing technology and using thicker elements, output power density above 10 W/cm^2 should be achievable.

The authors are grateful to Dr. Thierry Caillat for the variable temperature measurements of the electrical conductivity. We also acknowledge useful discussions with Dr. Mihai Gross. This work was supported by the Office of Naval Research Thermionic Energy Conversion Center MURI and ONR under Contract No. N00014-05-1-0611.

¹D. M. Rowe, *Thermoelectrics Handbook: Macro to Nano* (CRC, New York, 2005).

²L. D. Hicks and M. S. Dresselhaus, *Phys. Rev. B* **47**, 12727 (1993).

³G. Zeng, J. M. O. Zide, W. Kim, J. E. Bowers, A. C. Gossard, Z. Bian, Y. Zhang, A. Shakouri, S. L. Singer, and A. Majumdar, *J. Appl. Phys.* **101**, 034502 (2007).

⁴A. Shakouri and J. E. Bowers, *Appl. Phys. Lett.* **71**, 1234 (1997).

⁵D. Vashaee and A. Shakouri, *Phys. Rev. Lett.* **92**, 106103 (2004).

⁶M. V. Simkin and G. D. Mahan, *Phys. Rev. Lett.* **84**, 927 (2000).

⁷S. T. Huxtable, A. R. Abramson, C. L. Tien, A. Majumdar, C. LaBounty, X. Fan, G. Zeng, J. E. Bowers, A. Shakouri, and E. T. Croke, *Appl. Phys. Lett.* **80**, 1737 (2002).

⁸R. Venkatasubramanian, E. Siivola, T. Colpitts, and B. O'Quinn, *Nature (London)* **413**, 597 (2001).

⁹W. Kim, S. L. Singer, A. Majumdar, D. Vashaee, Z. Bian, A. Shakouri, G. Zeng, J. E. Bowers, J. M. O. Zide, and A. C. Gossard, *Appl. Phys. Lett.* **88**, 242107 (2006).

¹⁰W. Kim, J. Zide, A. Gossard, D. Klenov, S. Stemmer, A. Shakouri, and A. Majumdar, *Phys. Rev. Lett.* **96**, 045901 (2006).

¹¹D. C. Driscoll, M. Hanson, C. Kadow, and A. C. Gossard, *Appl. Phys. Lett.* **78**, 1703 (2001).

¹²D. C. Driscoll, M. P. Hanson, E. Mueller, and A. C. Gossard, *J. Cryst. Growth* **251**, 243 (2003).

¹³J. M. Zide, D. O. Klenov, S. Stemmer, A. C. Gossard, G. Zeng, J. E. Bowers, D. Vashaee, and A. Shakouri, *Appl. Phys. Lett.* **87**, 112102 (2005).

¹⁴J. M. O. Zide, D. Vashaee, Z. X. Bian, G. Zeng, J. E. Bowers, A. Shakouri, and A. C. Gossard, *Phys. Rev. B* **74**, 205335 (2006).

¹⁵X. Fan, "Silicon Microcoolers," Ph.D. thesis, University of California, Santa Barbara, 2002.

¹⁶C. LaBounty, "Heterostructure Integrated Thermionic Cooling of Optoelectronic Devices," Ph.D. thesis, University of California, Santa Barbara, 2001.

¹⁷J. M. O. Zide, "Molecular Beam Epitaxial Growth of III-V Semimetal/III-V Semiconductor Nanocomposites for Energy Conversion Applications," Ph.D. thesis, University of California, Santa Barbara, 2007.